Published in final edited form as:
Biochemistry. 2011 May 17; 50(19): 3879–3890. doi:10.1021/bi101702c.

Cardiolipin-Deficiency in *Rhodobacter sphaeroides* Alters the Lipid Profile of Membranes and of Crystallized Cytochrome Oxidase, but Structure and Function are Maintained†

Xi Zhang[1,2,3], **Banita Tamot**[1,3], **Carrie Hiser**[1], **Gavin E. Reid**[1,2], **Christoph Benning**[1], and **Shelagh Ferguson-Miller**[1,*]

[1] Department of Biochemistry and Molecular Biology, Michigan State University, East Lansing, MI 48824

[2] Department of Chemistry, Michigan State University, East Lansing, MI 48824

Abstract

Many recent studies highlight the importance of lipids in membrane proteins, including in the formation of well-ordered crystals. To examine the effect of changes in one lipid, cardiolipin, on the lipid profile and the production, function and crystallization of an intrinsic membrane protein, cytochrome *c* oxidase, the cardiolipin synthase (*cls*) gene of *Rhodobacter sphaeroides* was mutated, causing > 90% reduction in cardiolipin content *in vivo* and selective changes in the abundances of other lipids. Under these conditions, a fully native cytochrome *c* oxidase (C*c*O) was produced, as indicated by its activity, spectral properties and crystal characteristics. Analysis by MALDI tandem mass spectrometry (MS/MS) revealed that the cardiolipin level in C*c*O crystals, as in the membranes, was greatly decreased. Lipid species present in the crystals were directly analyzed for the first time using MS/MS, documenting their identities and fatty acid chain composition. The fatty acid content of cardiolipin in *R. sphaeroides* C*c*O (predominantly 18:1) differs from that in mammalian C*c*O (18:2). In contrast to the cardiolipin-dependence of mammalian C*c*O activity, major depletion of cardiolipin in *R. sphaeroides* did not impact any aspect of C*c*O structure or behavior, suggesting a greater tolerance of interchange of CL by other lipids in this bacterial system.

Lipids are resolved in the crystal structures of many membrane proteins, implying a significant role in protein structure and function (1, 2). Specific lipids have been shown to be required for correct folding and assembly of several membrane proteins including the plant light harvesting complex (3) and the bacterial lactose permease (4–6). Other studies on bovine and yeast cytochrome bc_1, bovine cytochrome *c* oxidase, and bacterial KcsA K^+ channel indicate a requirement for specific lipids for full activity (7–12). In some cases, complete removal of bound lipid *in vitro* results in abolishment of protein function, an effect that is reversed by adding back certain types of lipids (11–13). Investigating the roles of bound lipids is therefore an important part of understanding the mechanism and regulation of membrane proteins.

†The work was supported by NIH R01 GM26916 (SFM) and the Michigan State University Center of Excellence for the Structural Analysis of Membrane Proteins (CB, GER and SFM).

*Corresponding author: Shelagh M. Ferguson-Miller, Ph. D., Department of Biochemistry and Molecular Biology, Michigan State University, East Lansing, MI 48824, Phone: (517) 353-3512, Fax: (517) 353-9334, fergus20@msu.edu.
[3]These authors contributed equally to this work.

Supporting Information
Supporting information can be found at http://pubs.acs.org.

Lipids are found to stabilize membrane protein structure (14) and therefore retention of lipid molecules during purification has been emphasized as an important factor in the successful crystallization of membrane proteins (2, 15). The observation that the quality of *E. coli* lactose permease crystals can be controlled by changing the phospholipid content (16) demonstrates this principle. Similarly, the crystallization of the cytochrome b_6f complex was improved by the addition of lipids (14). Efforts to obtain high resolution structures of membrane proteins thus demand a closer scrutiny of the role of protein-associated lipid molecules.

The terminal enzyme of the respiratory electron transport chain, cytochrome *c* oxidase (C*c*O) (17, 18), has served as a model system for studying the involvement of lipids in membrane protein structure and function (19, 20) because its spectrally-accessible metal centers provide sensitive intrinsic probes for monitoring structural integrity and activity. A number of lipid molecules co-purify with C*c*O from bovine heart and *R. sphaeroides* and the lipid binding sites identified crystallographically in the core subunits of C*c*O are highly conserved from bacteria to mammals (2, 21, 22), suggesting an important role not only in function but also in achieving high resolution crystal structures of C*c*O.

Cardiolipin (CL) is one lipid whose requirement has been established by biochemical studies of a number of membrane proteins, particularly respiratory chain complexes from both bacterial and mitochondrial sources (7, 10, 11, 23, 24). Its unique structure, composed of two phosphates, three glycerols and four hydrophobic fatty acid chains, enables cardiolipin to bind to membrane proteins more tenaciously than lipids with only two alkyl chains. Recent evidence suggests that it can act as a glue between proteins that form super-complexes in membranes (25, 26) and that it plays a role in the signaling system that controls apoptosis in eukaryotic cells (27, 28). It has also been reported to be essential for the full activity of mammalian heart C*c*O (7, 29), but most of these studies removed CL *in vitro* after the enzyme was purified. In contrast, several *in vivo* studies in yeast report that a deficiency in cardiolipin did not significantly affect the activity of C*c*O, nor did it alone cause mitochondrial dysfunction (30–32). However, the deficiency of both phosphatidylglycerol (PG) and CL resulted in very little C*c*O production and severely dysfunctional mitochondria (30), suggesting CL is functionally replaceable by PG but not other lipids in yeast.

To test if CL is strictly required in C*c*O from the purple non-sulfur bacterium *R. sphaeroides*, C*c*O was expressed in a CL-deficient mutant created by deleting the *cls* gene encoding CL synthase. The expression, activity, structure, crystallization, and lipid composition of C*c*O were examined. The results support a flexible lipid requirement in this bacterial enzyme.

Materials and Methods

Media and growth conditions

All *R. sphaeroides* strains were grown in Sistrom's succinate-basal salts medium (33, 34). The cells were grown on agar-solidified medium or in liquid cultures at 30 °C under anaerobic photoheterotrophic (35) or aerobic chemoheterotrophic (36) conditions, as previously described. When required, ampicillin (50 μg/mL), kanamycin (25 μg/mL), tetracycline (1 μg/mL), chloramphenicol (25 μg/mL), streptomycin (5 μg/mL) or spectinomycin (5 μg/mL) was added to the media. *Escherichia coli* cells were grown in LB medium at 37 °C and, when required, antibiotics were added to the solid media or liquid cultures at the concentration of 50 μg/mL of ampicillin, kanamycin or chloramphenicol.

For photosynthetic growth curves, 2.4.1 (wild-type, CL+) (37) and CL3 (*cls* deletion, CL−) strains were grown in 250 mL sidearm flasks filled completely with Sistrom's medium under approximately 30 μmol m^{-2} s^{-1} light without shaking. For aerobic growth curves, strains 2.4.1 and CL3 were grown at 30 °C in 50 mL of Sistrom's medium in 250 mL sidearm flasks with vigorous shaking (250 rpm). In each case, cell densities were measured in a Klett photometer with a #66 filter. Note that 1 Klett unit is equivalent to 10^7 cells per mL (38).

Construction of plasmid pSUP-CLD

Using genomic DNA from the wild-type strain 2.4.1 as a template, a 600 nucleotide region of the *cls* gene (GenBank YP_353546 coding sequence, nucleotides 1 to 600) was PCR amplified using the primers P1, 5′-GCGGGATCCATGATCGACGACTGGCTGGGCGTCC - 3′, and P3, 5′-GCGGTCGACGTTGCGCCCGCCCACGATGGCC - 3′, *Sal*I. Similarly, a 591 nucleotide region of the gene (GenBank YP_353546 coding sequence, nucleotide 961–1551) was amplified by using another set of primers, P2, 5′-GCGAAGCTTGGATCCTCAGAGGTAGCTCTGGATCG - 3′, *Hind*III, *Bam*HI and P4, 5′-GCGGTCGACGGCGAGGCGATCACCGCGCTCC - 3′, *Sal*I. The amplified products were cloned into the vectors pPICT-2 and pGEM-T Easy (Promega, Madison, WI), respectively, to generate the plasmids pPICT-2-I and pGEM-T-II. Segment II from the plasmid pGEM-T-II was cut out by double digestion with *Sal*I and *Hind*III and was ligated into pPICT-2-I which had been digested with the same enzymes to generate the plasmid pPICT-2-I/II. From the pUC4K plasmid (GE Healthcare, Piscataway, NJ), the kanamycin resistance cassette (*kan*R) was cut out by using *Sal*I sites placed on either side of the gene and was subsequently inserted into the plasmid pPICT-2-I/II which had been digested by the same enzymes. The resulting plasmid pPICT-2-CK contained the *kan*R cassette inserted between segments I and II. The orientation of *kan*R was checked by digesting the plasmid pPICT-2-CK with *Hind*III. Since a *Hind*III site is placed asymmetrically within *kan*R, digestion by the enzyme would produce fragments of different sizes based upon the orientation of the gene (39). Using *Bam*HI, the entire gene construct was cut out from the plasmid pPICT2-CK and was ligated into the suicide plasmid pSUP202 (40) by using the *Bam*HI site placed within the tetracycline resistance gene, to obtain the plasmid pSUP-CLD.

Disruption of the cls gene in R. sphaeroides 2.4.1

The plasmid pSUP-CLD was mobilized into the wild-type strain 2.4.1 (39) by using the *E. coli* strain S17-1 (RP4-2-Tc::Mu-Km::Tn7Tp $^{r}Sm^{r}Pro^{-}$; (40)) as a donor. Through selection for kanamycin (100 μg/mL) resistance, the plasmid was forced to recombine with the genome using the regions homologous to *cls* gene. The exconjugants with double crossovers were selected by ampicillin and chloramphenicol sensitivity (39). The resulting mutant strain of *R. sphaeroides* was called CL3. The gene disruption in the mutant was verified by PCR.

Quantitative membrane lipid analysis using TLC and radioactive labeling

Cultures of wild-type and mutant strains were grown aerobically overnight. Lipids were then labeled by incubating the cultures with [1-^{14}C]-acetate as described (41). Cells were collected by centrifugation and washed twice and suspended in 50 μL water. From the cells, lipid extracts were prepared and loaded onto activated silica thin-layer chromatography (TLC) plates (Si250; Baker) as previously described (35). The lipids were separated by two-dimensional TLC using chloroform-methanol-water (65:25:4, v/v/v) for the first dimension and chloroform-methanol-acetic acid-water (170:25:25:4 v/v/v/v) for the second dimension. Lipids were visualized by charring with 50% H_2SO_4 (42). The plates were then exposed to a phosphoimager (GE Healthcare) to obtain an image of the labeled lipids. The lipids on the

TLC plates were then visualized by iodine staining and the radioactivity in the individual spots was measured by using a liquid scintillation counter (41). The relative amount of each lipid was calculated as the percentage of total radioactivity present in the lipid sample.

Engineering R. sphaeroides 2.4.1 and CL3 strains to overproduce CcO

To overproduce a histidine-tagged version of the C*c*O enzyme, the pRK-pYJ123H plasmid (36) carrying the genes coding for a wild-type C*c*O was transferred by conjugation from *E. coli* S17-1 into *R. sphaeroides* strains 2.4.1 and CL3 as described (36) to create strains 2.4.1+C*c*O (CL+) and CL3+C*c*O (CL−), respectively. These strains were grown aerobically in Sistrom's media containing 1 μg/mL tetracycline.

To overproduce a version of C*c*O suitable for crystallization, a histidine tag on subunit II and a shortened version of subunit IV are required to improve molecular homogeneity (2). Therefore, the pCH169 plasmid (2) carrying these versions of the C*c*O genes was transferred by conjugation into the CL3 mutant strain to create strain 169/CL3 (Supplemental Table S1). The CL(+) crystallography strain used as the control herein is 169, which is derived from a 2.4.1 C*c*O deletion strain (YZ200, (36)) and carries the pCH169 plasmid (2).

The lipid composition of the membranes from the two different strains without the *cls* deletion (2.4.1+C*c*O and 169, both refered to as WT or as CL(+)) were found to be the same, by mass spectrometry lipid analysis. Similarly the two strains carrying the *cls* deletion (CL3+C*c*O and 169/CL3, both refered to as CL(−)) also showed the same lipid profile (data not shown), as expected since these strains are derived from the same parent strain, CL3 (43). All strains used for C*c*O production in this study are listed in Supplemental Materials Table S1.

CcO purification, characterization and crystallization

R. sphaeroides strains overexpressing 6xhistidine-tagged C*c*O were grown aerobically in Sistrom's medium with appropriate antibiotics as described (36). C*c*O protein was purified by using nickel affinity chromatography and monitored by UV-Vis spectroscopy (dithionite-reduced minus ferricyanide-oxidized or dithionite-reduced only) (36). C*c*O protein for crystallization was purified as described previously (2). Maximal rates of oxygen consumption by purified C*c*O were measured polarographically in 50 mM KH_2PO_4 pH 6.5 with 0.05% (m/v) lauryl maltoside, 1 mM *N*,*N*,*N*′,*N*′-tetramethyl-*p*-phenylenediamine (TMPD), 2.8 mM ascorbate, and 30 μM cytochrome *c* as the substrate and in the absence or presence of externally-added lipids (a mixture of soybean asolectin at final concentration of 0.44 mg/mL (Avanti Polar Lipids, Alabaster, AL) and cholate at final concentration of 0.02%). The enzymatic activity (turnover number; moles cytochrome *c* oxidized per mole enzyme per second) was calculated as described (44). Total protein amounts were determined by using the bicinchroninic acid protein assay kit (Pierce, Rockford, IL) including 0.25% deoxycholate in the buffer (45). Four subunit and two subunit C*c*O protein crystals were obtained using methods described earlier (46) from the crystallization optimized strains.

Direct mass spectrometry analysis of lipids in membranes and protein crystals

Mass spectrometry (MS) and tandem mass spectrometry (MS/MS) analysis of lipids in the isolated membranes and C*c*O protein crystals were performed using a linear quadrupole ion trap mass spectrometer equipped with a vacuum matrix-assisted laser desorption/ionization ion source (model vMALDI-LTQ, Thermo Scientific, San Jose, CA). Protein crystals were rinsed briefly in water at 4 °C to remove residual protein precipitate and other well-solution components loosely attached to the surface of the crystals before re-dissolving them by extensive vortexing in water. One μL of either resuspended membrane (at a protein

concentration of 0.25 mg/mL determined by the BCA assay using bovine serum albumin as the standard) or 1 μL of redissolved C*c*O crystal solution (at a C*c*O concentration of 8.3 μM, equivalent to 1.00 mg protein/mL, determined by the BCA assay using purified C*c*O solution with a known concentration as the standard) were applied to individual spots on the stainless steel sample plate and dried in air. Subsequently, 1 μL of 0.1 M (for membrane samples) or 0.5 M (for crystal samples) 2,5-hydroxy benzoic acid (2,5-DHB, Sigma-Aldrich, Milwaukee, WI) dissolved in acetonitrile (Mallinckrodt Chemicals, Philipsburg, NJ): water (2:1, v/v) was added. MS and MS/MS spectra were acquired in negative and positive ion modes using enhanced resonance ejection scan conditions. MS/MS spectra were acquired using collision-induced dissociation (CID) typically at a normalized collision energy of 30%, an isolation width of 1.0 or 1.2, and an activation Q value of 0.2. The spectra shown were the average of 250 scans.

Results

Identification of a gene encoding CL synthase in R. sphaeroides

Since the gene encoding CL synthase (*cls*) had not been previously identified in *R. sphaeroides*, the candidate *cls* gene of *R. sphaeroides* (GenBank Protein ID YP_353546) was selected based on similarity to the amino acid sequence of *E. coli* CL synthase (27% identity, 44% similarity using BLAST (47)). The candidate gene was cloned into the *E.coli* expression plasmid pQE-30 (Qiagen, Valencia, CA) and transformed into the *E. coli* CL-deficient strain SD9 (48). Thin layer chromatograms of extracts from the SD9 transformant harboring the *cls* expression plasmid showed the presence of CL while no CL was observed for SD9 transformed with empty vector (43). These results suggest that the *R. sphaeroides cls* gene functionally complements the *E. coli* CL-deficient mutant and thus encodes a CL synthase of *R. sphaeroides*.

Construction of R. sphaeroides CL synthase mutant

The genomic copy of the *cls* gene was replaced by a disrupted copy carried by the plasmid pSUP-CLD to obtain a CL synthase-deficient mutant of *R. sphaeroides* (Figure 1A). Gene disruption was confirmed by PCR analysis of genomic DNA. The PCR amplification using the primers specific for the two ends of the *cls* gene (P1 and P2) gave a larger amplified product in the mutant compared to the wild type (Figure 1B). The size of the amplified product in the mutant (approximately 2.6 kb) equaled the sum of the sizes of the kanamycin resistant cassette (1.2 kb) plus the 5′ region (0.6 kb) and 3′ region (0.59 kb) of the *cls* gene that had been amplified and used for obtaining the gene disruption construct. A second PCR using the *cls* gene specific primer P2 and the kanamycin resistant gene specific primer P5 gave a product of the expected size (approx. 0.96 kb) in the mutant, whereas no amplification was seen in the wild type (Figure 1B). TLC analysis of the lipid extracts from the wild type and the mutant (designated CL3) showed a strong reduction in the level of CL in the mutant (Figure 2). The result clearly indicated that the inactivation of the *cls* gene impaired CL synthesis in the mutant.

Composition of general lipid types in the wild type and the mutant cells

To determine the effect of *cls* gene inactivation on lipid content, a saturation ^{14}C-acetate labeling approach was used to obtain a quantitative comparison of relative lipid amounts in the wild type and the CL3 mutant. The level of CL in the mutant was strongly reduced, but a trace of CL, less than 10% of wild type, was still present in the mutant (Table 1). The result was consistent with that observed for an *E. coli cls* knockout mutant, in which a low level of CL was also still present (49). Corresponding to the decrease in CL in the CL3 mutant, an increase in PG, the precursor for CL synthesis, was observed (Table 1). Within statistical limitations, the amounts of phosphatidylcholine (PC), phosphatidylethanolamine (PE),

ornithine lipid (OL) and sulfoquinovosyldiacylglycerol (SQDG) remained relatively unchanged. The structures of the molecular species in each type of lipid in the cell membranes were elucidated by MALDI MS and MS/MS as well as ESI MS, MS/MS and multistage tandem mass spectrometry (MS^n) in the linear ion trap mass spectrometer (50). The changes in the amounts of the phospholipids revealed by TLC were confirmed by quantitative ESI analysis of the phospholipids using internal standards in both MS and MS/MS (see accompanying paper).

Effect of CL deficiency on R. sphaeroides cell growth

To analyze the effect of the decreased CL on the overall growth of *R. sphaeroides* cells, the photosynthetic and respiratory growth of the wild-type and the mutant was compared. Under the conditions used in this study, no significant differences were observed in the photosynthetic growth for both lines (Figure 3A). Respiratory growth was slightly reduced in the mutant, as indicated by the increased lag time (slower approach to final cell density) and lower final cell density (Figure 3B). The results suggest that CL may contribute to optimal respiratory growth, but may be less critical to photosynthetic growth.

Production of CcO in R. sphaeroides wild-type and CL-deficient cells

The wild-type 2.4.1 strain of *R. sphaeroides* naturally produces a low level of C*c*O in its membranes when grown under aerobic conditions (Figure 4A). Since this strain has been previously used to produce a variety of lipid mutants (39, 42, 51), it was necessary to demonstrate that it is also a suitable host for C*c*O overproduction to provide the model system for testing the role of lipids in this protein. Optical difference spectra of reduced minus oxidized states provide a facile method to assess the level of C*c*O in the membrane by the absorbance of its *a*-type hemes. Difference spectra of the solubilized membrane proteins of the wild-type 2.4.1 strain (Figure 4A) showed that the 606 nm peak, representing *a*-type hemes of C*c*O, was much smaller than the 560 nm peak to which the spectra are normalized. (Note that the 560 nm peak represents *b*-type hemes of the bc_1 complex plus a *cbb*3 oxidase also present in the membranes. In addition, a membrane-bound cytochrome *c* contributes to the 550 nm region.) After the C*c*O genes were introduced on the plasmid pRK-pYJ123H to create strain 2.4.1+C*c*O, the 606 nm peak was strongly increased relative to the 560 nm peak, indicating an overproduction of C*c*O (Figure 4B). This was confirmed by measuring the concentration of C*c*O per mg total protein, which showed an equivalent increase. When this plasmid was introduced into the CL-deficient strain CL3, high levels of C*c*O expression were also seen, but were variable depending on the culturing time and volume of the culture (data not shown). In smaller volume cultures the levels of C*c*O were high, while they were sometimes lower in larger cultures grown for longer times. This observation indicates a possibly greater sensitivity of the CL3 mutant to the stress experienced during subculturing and dilution into larger flasks (see also accompanying paper).

Properties of CcO purified from wild-type and cls mutant cell lines

Table 2 lists the spectral properties and enzymatic activities of C*c*O protein purified from *R. sphaeroides* cell lines overproducing a histidine-tagged version of C*c*O. The Soret (445 nm) and alpha (606 nm) bands in the optical spectra are diagnostic of the native, reduced heme centers of C*c*O. No wavelength shifts of peak maxima were observed between the CL(−) mutant cell line (CL3+C*c*O) and the CL(+) control (2.4.1+C*c*O), indicating that the absence of the *cls* gene in the mutant did not impair its ability to correctly assemble and insert the metal centers into C*c*O. The enzymatic activities of C*c*O purified from CL(−) and CL(+) strains were also very similar, indicating that the enzyme purified from the CL(−) mutant cells was as active as that purified from the CL(+) cells. The activities of all purified C*c*Os increased similarly in the presence of externally-added lipids during the assay. This commonly observed phenomenon is likely related to the extent of delipidation of C*c*O

during the purification process (44). When tested for stability at temperatures ranging from 20 °C to 80 °C, C *c*O purified from both the wild-type and mutant strains behaved similarly (data not shown).

SDS-PAGE analysis of C*c*O purified from CL(+) and CL(−) mutant strains indicated that the composition and relative levels of all of the subunits were similar (see accompanying paper).

MALDI MS analysis of lipids in the membranes overexpressing CcO

Figure 5(A and B) shows the negative ion mode MALDI MS spectra of the lipids in the isolated membranes of the CL(+) and CL(−) strains of *R. sphaeroides*. Similar types of lipids were observed in the membranes of both strains, including PE, PG, SQDG, and CL, although with varying abundance. The major molecular species of lipids detected in these strains include the phospholipids PE 18:1/18:1 (m/z 742.5), PG 18:1/18:1 (m/z 773.5), cardiolipins $CL(18:1)_4$ (m/z 1456.0), $CL(16:1)_1(18:1)_3$ (m/z 1428.0), $CL(16:0)_1(18:1)_3$ (m/z 1430.0) and $CL(18:0)_1(18:1)_3$ (m/z 1458.0), as well as sulfolipids SQDG 16:0/16:0 (m/z 793.5), SQDG 16:0/18:1 (m/z 819.5), SQDG 16:0/18:0 (m/z 821.5), SQDG 18:1/18:1 (m/z 845.5) and SQDG 18:0/18:1 (m/z 847.5). The identities of each of the membrane lipid species labeled in these figures were confirmed by MS/MS analysis (50). Note that although MALDI is not generally considered to be a rigorously quantitative method due to issues arising from matrix/sample heterogeneity, these experiments were performed in parallel under identical sample handling and data acquisition conditions and in multiple replicates, giving confidence in a semi-quantitative interpretation of the data, particularly using MS/MS, since the chemical noise observed during MS analysis is mostly eliminated (52). Further, MALDI has the major advantage of being able to analyze samples directly, without chemical solvent extraction, and being more tolerant of the presence of detergent than ESI, thus bypassing problems caused by detergents and detergent removal procedures (50). These facts, along with the good agreement with the radioactive labeling analysis (Table 1) and quantitative ESI measurements described in Figures 2 and 4 of the accompanying paper, lend strength to the quantitative significance of the observation of approximately 5% relative abundance of CL ions in CL(−) membranes compared to the CL(+) membranes. The 5% level is calculated relative to the ion abundances of PE 18:1/18:1 at m/z 742.5 and SQDG 18:1/18:1 and SQDG 18:0/18:1 at m/z 845.5 and 847.5, the most abundant ions within the displayed m/z range (Figures 5A and 5B). In contrast, the abundance of the PG 18:1/18:1 (m/z 773.5), and the SQDG 16:0/18:1 and SQDG 16:0/18:0 lipid species (m/z 819.5 and 821.5, respectively), showed an apparent increase in the CL(−) mutant membrane. (It should be noted that the m/z 1495.9 and m/z 1497.9 ions seen in negative ion mode were determined not to be related to cardiolipin by MS/MS and MS^3 analysis.)

The positive ion mode MALDI MS spectra of the membranes of the CL(+) and CL(−) strains are shown in Figures 5C and 5D. In addition to the most abundant PC lipid ions (PC 18:1/18:1 [m/z 786, 808, 824], PC 18:1/19:1 [m/z 800, 838]), PE lipids (mainly PE 18:1/18:1 [m/z 744, 766]) and ornithine lipids (OL 3-OH 20:1/19:1, m/z 719) were also observed in positive ion mode. The recently discovered glutamine lipids (QL) (53) were also identified by ESI analysis of the membrane lipid extract (supplementary of accompanying paper); QL has a relatively lower ionization efficiency in MALDI and overlaps with the m/z 719 of OL. Comparison of Figure 5C with Figure 5D suggests that PC, PE and OL are not significantly affected by the *cls* mutation, either in molecular structural diversity or in relative quantity.

Purification and crystallization of CcO from wild-type and cls mutant

The *R. sphaeroides* strain containing the *cls* deletion and a plasmid containing C*c*O designed for crystallization (169CL3) displayed high expression yield. The UV-Vis spectral characteristics of the C*c*O purified from this CL(−) strain, in reduced and oxidized forms, were essentially identical in the peak positions of the hemes *a* and a_3 to those of the C*c*O obtained from the CL(+) strain purified in the same manner (Figure 6).

The C*c*O purified from CL(+) and CL(−) strains contained the normal four subunits (I, II III and IV) as revealed by SDS-PAGE analyses (see accompanying paper). Using C*c*O purified from CL(+) and CL(−) strains, C*c*O crystals were obtained with four subunits and with two-subunits (subunit I and II only) for both strains, under the same crystallization conditions and yielding the same form (space group $P2_12_12_1$ for 2-subunit crystal; R3 for 4-subunit crystal). The resolution obtained for the four-subunit C*c*O crystals from the CL(−) mutant (3.2 Å) was similar to that of four-subunit crystals from the CL(+) strain (3.3 Å), while the resolution for the 2-subunit crystals from the CL(−) mutant (3.3 Å) was slightly less than that from the CL(+) strain (2.9 Å) based on many repeats with the CL(+) and CL(−) forms, grown, purified and crystallized in parallel over several years (Supplemental Table S2). Thus, the strongly decreased levels of CL observed in the membrane lipid profile did not prevent the crystallization of four-subunit or two-subunit C*c*O. The four-subunit C*c*O crystals generated were examined by MALDI MS and MS/MS analysis.

MALDI MS and MS/MS analysis of the lipids in the re-dissolved four-subunit CcO crystals

Figure 7 shows the MALDI MS spectra obtained by direct analysis of the re-dissolved crystals, in negative ion mode (Figures 7A and 7B) and in positive ion mode (7C and 7D).

The data show that C*c*O crystals from the CL(+) strain retain readily detectable and multiple species of CL and SQDG, as well as PG 18:1/18:1, and OL 3-OH 20:1/19:1 in negative ion mode (Figure 7A), PC18:1/18:1 and PE18:1/18:1 in positive ion mode, as confirmed by MS/MS analysis (Figures 8 and 9). These detailed structures of the lipids in the crystals have not been previously reported. Both cardiolipin and SQDG contained multiple fatty acid chain compositions. In addition to the most abundant $CL(18:1)_4$ (m/z 1456), minor species of $CL(16:1)_1(18:1)_3$ (m/z 1428) and $CL(16:0)_1(18:1)_3$ (m/z 1430) were also found, in ratios similar to those found in the membrane, indicating no apparent selection for CL on the part of C*c*O during purification and crystallization. SQDG in the crystals also included a variety of fatty acid chain compositions (Figures 9B and 9C), all at comparable relative abundance. The relative levels of various fatty acids appear to be representative of the membrane background (compare Figure 7 and Figure 5), suggesting that C*c*O also has little selectivity for fatty acid chain variations in SQDG.

In the C*c*O crystals from the CL(−) mutant, MS clearly reveals significantly decreased levels of CL (Figure 7B) equivalent to those in the CL(−) membrane (Figure 5B), as well as apparently higher abundance of SQDG species (m/z 793, 819, 821, 845, 847) compared to the CL(+) crystal (Figure 7A). MS/MS further demonstrates that the level of $CL(18:1)_4$ (m/z 1456) in the CL-deficient mutant crystal is about ~10% of that seen in the wild type, as indicated by comparison of the absolute abundances of the m/z 699 fragment ion (the 18:1/18:1 phosphatidyldioleoylglyceride ion) (50, 54) in the MS/MS spectra of the m/z 1455.9 precursor ions from CL(−) and CL(+) crystals (Figures 8A and 8B). These results are again consistent with the membrane CL levels and with radioactive labeling (Table 1), suggesting no strong selectivity of C*c*O for CL in a CL(−) membrane environment. The PG lipid species (m/z 773.5) show increase in abundance to some extent, while PE, PC and OL lipids are observed in MS positive ion mode to be at similar relative levels to those in the crystals of the CL(+) strain (Figures 7C and 7D).

It is noteworthy that the major molecular species of cardiolipin in the isolated cell membranes and the C*c*O crystals of *R. sphaeroides* has four 18:1 fatty acyl chains $CL(18:1)_4$ (m/z 1456) and the three minor species of cardiolipin are $CL(16:1)_1(18:1)_3$, $CL(16:0)_1(18:1)_3$ and $CL(18:0)_1(18:1)_3$. However, $CL(18:2)_4$ (tetralinoleoyl cardiolipin; m/z 1448), the predominant cardiolipin species found in mammalian mitochondria (29, 55), was not observed in any of the samples of *R. sphaeroides* examined in the current study.

Discussion

Residual CL in the cardiolipin-deficient mutant

The *cls*-encoded enzyme catalyzes the synthesis of CL from two PG molecules (56). Although lipid analysis showed a significant reduction in the level of CL in the mutant membranes, a low amount of CL (<10% wild-type) still persisted in both the membrane and the C*c*O crystals of the mutant, as confirmed by saturation radioactive labeling, MALDI MS, MALDI MS/MS, and ESI with internal standards (accompanying paper). At this reduced CL level, no appreciable effects were observed on the protein expression, protein spectroscopic properties, activity, assembly and crystallization.

The source of this residual CL in the mutant still needs to be determined. In the *E. coli cls* knockout mutant, overexpression of the *pss* gene led to an increase in the CL level (49), suggesting that phosphatidylserine synthase has CL synthase activity. In a similar experiment, it has been observed that the expression of the *pss* gene (GenBank protein ID YP_353797) from *R. sphaeroides* in the *E. coli* SD9 strain resulted in the synthesis of CL (up to 1%) which showed dependence on the level of expression of the gene (43). Thus, as observed for *E. coli*, phosphatidylserine synthase may be the source of the residual CL in the CL3 mutant of *R. sphaeroides* (43).

Difference between molecular components of CL in R. sphaeroides and mammalian cells

Mass spectrometry analysis revealed that the CL molecular species in the membrane, the purified C*c*O enzymes, and the C*c*O protein crystals, is mainly $CL(18:1)_4$, while much less abundant $CL(16:1)_1(18:1)_3$, $CL(16:0)_1(18:1)_3$ and $CL(18:0)_1(18:1)_3$ were also present. In contrast to the mammalian mitochondria, where $CL(18:2)_4$ is the predominant and functionally essential species (29, 55, 57), the *R. sphaeroides* contained no $CL(18:2)_4$ detectable by MS. One important role of cardiolipin in mammalian mitochondria has been proposed to be a part of the signaling system in apoptosis, involving the peroxidizability of the 18:2 unsaturated fatty acyl chains and not the 18:1 acyl chain components (29, 55, 58). The predominant CL species in healthy mammalian mitochondria is $CL(18:2)_4$, and a relative decrease of the 18:2 cardiolipin component has been correlated with diseased mitochondria (29, 55). CL $(18:2)_4$ is also found to activate mammalian C*c*O more efficiently than other lipids (59). Notably, $CL(18:2)_4$ is not synthesized directly in mammalian cells, but is formed through a modification by acyltransferases of the initial cardiolipin species (58), a process that is absent in the bacterial systems (58, 60). Yeasts also predominantly produce cardiolipin containing 16:1 and 18:1 fatty acyl chains but not 18:2 (61, 62). The observed difference in cardiolipin types may account for fundamental differences in the functional roles that cardiolipin plays in the bacterial, yeast, and mammalian systems.

CL and growth of R. sphaeroides

The CL3 mutant showed some decreased growth under respiratory conditions, suggesting that a normal level of CL is important for robust respiratory growth. A similar effect of CL deficiency on respiratory growth has been observed in a *Saccharomyces cerevisiae crd1*Δ mutant, in which the loss of CL affects the stability of the respiratory chain complexes (25, 26, 63). The photosynthetic growth of the CL3 mutant was not affected, probably because

other lipids such as PG substituted for CL. It has been shown that PG is preferentially increased in purple bacteria during photosynthetic growth (64). It is possible that the level of CL needed for photosynthetic growth is not as high as that needed for respiratory growth, and therefore the low level of CL retained by the CL3 mutant could be sufficient under photosynthetic conditions.

Alternatively, CL may be only required during stress situations. Osmotic stress during growth has been shown to increase CL synthesis in *R. sphaeroides* (65). Variable, but often lower, levels of C*c*O production are observed from CL3 cultures, a response which may be due to the added stress of subculturing, dilution and growth at high oxygen levels and high pH (approaching stationary phase). Determining a specific role of CL during respiratory growth in *R. sphaeroides* will require further studies.

CL in the function and assembly of CcO of R. sphaeroides

Low levels of CL did not appreciably affect the assembly or the activity of the purified enzyme (Table 2). The C*c*O produced the same type of four-subunit crystals which diffracted to the same level as crystals from the CL(+) strains (Table S2). It was critical to determine whether, despite the low CL levels, C*c*O was able to preferentially sequester enough CL for its needs. However, the MS and MS/MS analyses reproducibly demonstrated that the purified enzyme and the crystals did not concentrate CL above that found in the membranes. It is reasonable to conclude that CL is not essential for the structure, function or crystallization of *Rhodobacter* C*c*O, consistent with several previous studies using bacterial and yeast systems (30–32). This is in contrast to numerous biochemical and biophysical studies which suggest a requirement for CL in mammalian systems (7, 29, 58, 66).

A CL requirement for maintaining supercomplexes between C*c*O and other membrane proteins of the respiratory chain, and not for the stability or activity of C*c*O per se, could still be the case in *R. sphaeroides*, since evidence of such complexes are also found in other bacterial systems (67). Experiments in yeast suggest that complexes III (bc_1) and IV (C*c*O) do not form the normal level of supercomplexes in the mitochondria of CL-deficient mutants, and CL-deficient yeast cultures also grew more slowly and to a lower final density than wild-type yeast cultures (25). Similarly, the CL3 mutant showed slower growth under respiratory conditions in this study (Figure 3) but no direct evidence is available to support a role in supercomplex formation.

The mass spectrometric data on C*c*O suggests that other lipids may functionally substitute for CL in *R. sphaeroides*. A relative increase in the levels of SQDG and PG was observed in crystals from the CL(−) mutant strain (Figure 7B). The increase in PG in the CL(−) mutant was also observed in the membrane samples by radioisotope labeling (Table 1). Earlier studies comparing the yeast *cls* mutant (CL-deficient) and *pgs* mutant (PG and CL-deficient) suggested that CL is not essential for the functions of C*c*O or mitochondria in yeast (30–32), but can be functionally replaced by PG (30). The lack of difference in SQDG levels observed in membrane preparations, when analyzed either by thin-layer chromatography or by mass spectrometry, suggests that the altered levels seen in the crystals by MS may reflect some selectivity of C*c*O, rather than a general metabolic response at the cellular level. Specifically bound SQDG molecules have been previously resolved in the crystals of cyanobacterial photosystem II (68, 69) but not yet in *R. sphaeroides* C*c*O. The apparent increased abundance of SQDG in the C*c*O crystals suggests a possible compensatory role for SQDG during CL deficiency, since both are anionic lipids, and SQDG was found to increase in *R. sphaeroides* membranes under phosphate-limiting growth conditions (39). Studies in *Rhodobacter capsulatus*, which has neither CL nor an aa_3-type oxidase, have suggested a similar function for ornithine lipid (70). This type of lipid is present in the *R. sphaeroides*

membranes (53) but is not appreciably altered in CL(−) membranes, as seen by thin-layer chromatography and mass spectrometry.

In a previous study (2), high resolution (2.0 Å) two subunit C*c*O crystals were obtained which contain a potential CL binding site, based on homology with the bovine enzyme, even though the head group is not resolved. In the current study, the 2-subunit crystal form was produced from both CL(+) and CL(−) strains, but in neither case at high enough resolution to visualize the lipids, likely due to the background strain, 2.4.1, not containing the necessary deletion of subunit IV that has been found to be key to giving the highest resolution crystals (2).

Lipid mutants of R. sphaeroides as tools for the study of membrane proteins in vivo

One of the motivations for studying the production, properties, and crystallization of C*c*O in the CL-deficient mutant of *R. sphaeroides* was to test the hypotheses that 1) CL is a necessary component of the fully functional enzyme in *R. sphaeroides*; and 2) the specific lipid composition of a membrane protein sample is an important factor in achieving high quality crystals. The basis for the first hypothesis was a wealth of biochemical evidence supporting a role for CL in C*c*O function in mammalian systems (7, 12, 20, 66). The basis for the second hypothesis was the observation of specifically bound and conserved lipids in high resolution crystal structures of membrane proteins. A further motivation for these studies was to establish *R. sphaeroides* as a tool for the overproduction of membrane proteins from many sources for structural studies (71) by providing versions of *R. sphaeroides* with different and controlled lipid compositions.

The results herein, especially the MS lipid analysis of the C*c*O crystals, argue against both starting hypotheses and suggest that C*c*O in *R. sphaeroides* does not have a strict requirement for CL *per se*. The results demonstrate that it is possible to overproduce C*c*O in a CL-deficient mutant, and that the purified enzyme is fully active by available criteria and gives well-resolved crystals, despite a very low CL content. The ability to directly analyze the lipid content of the crystals provides unique insight into the effects of low CL, showing the presence of other bacterial lipids, including SQDG and ornithine lipid, apparently substituting for CL in the crystal. To determine the extent to which the roles of CL can be fully substituted by other lipid species in *Rhodobacter sphaeroides*, a method to further perturb the lipid profile and produce a more complete CL-deficiency was developed, using a combined metabolic and genetic approach (see accompanying paper).

Supplementary Material

Refer to Web version on PubMed Central for supplementary material.

Acknowledgments

We would like to thank Dr. Koichiro Awai for help with the design of the *cls* gene disruption strategy and Dr. Ling Qin for assistance in crystallizing C*c*O. We are grateful to Dr. Kouji Matsumato (Saitama University, Japan) for providing the *E. coli* CL-deficient mutant. Crystal screening was carried out at Argonne National Labs, APS synchrotron, LS CAT beamline.

Abbreviations

R. sphaeroides	*Rhodobacter sphaeroides*
C*c*O	cytochrome *c* oxidase
cls	cardiolipin synthase gene

CL	cardiolipin
PG	phosphatidylglycerol
PE	phosphatidylethanolamine
PC	phosphatidylcholine
OL	ornithine lipid
QL	glutamine lipid
SQDG	sulfoquinovosyldiacylglyceride
CL(+)	cardiolipin-proficient strain
CL(−)	cardiolipin-deficient strain
MALDI	matrix assisted laser desorption/ionization
nESI	nanoelectrospray ionization
MS	mass spectrometry
MS/MS	tandem mass spectrometry
MS^n	multistage tandem mass spectrometry
2,5-DHB	2, 5-hydroxybenzoic acid
SDS-PAGE	sodium dodecyl sulfate polyacrylamide gel electrophoresis
TLC	thin layer chromatography
PCR	polymerase chain reactions
WT	wild-type

References

1. Cherezov V, Rosenbaum DM, Hanson MA, Rasmussen SG, Thian FS, Kobilka TS, Choi HJ, Kuhn P, Weis WI, Kobilka BK, Stevens RC. High-resolution crystal structure of an engineered human beta2-adrenergic G protein-coupled receptor. Science. 2007; 318:1258–1265. [PubMed: 17962520]
2. Qin L, Hiser C, Mulichak A, Garavito RM, Ferguson-Miller S. Identification of conserved lipid/detergent-binding sites in a high-resolution structure of the membrane protein cytochrome c oxidase. Proc Natl Acad Sci U S A. 2006; 103:16117–16122. [PubMed: 17050688]
3. Nussberger S, Doerr K, Wang DN, Kuhlbrandt W. Lipid-protein interactions in crystals of plant light-harvesting complex. J Mol Biol. 1993; 234:347–356. [PubMed: 8230219]
4. Bogdanov M, Sun J, Kaback HR, Dowhan W. A phospholipid acts as a chaperone in assembly of a membrane transport protein. J Biol Chem. 1996; 271:11615–11618. [PubMed: 8662750]
5. Bogdanov M, Dowhan W. Phospholipid-assisted protein folding: phosphatidylethanolamine is required at a late step of the conformational maturation of the polytopic membrane protein lactose permease. Embo J. 1998; 17:5255–5264. [PubMed: 9736605]
6. Bogdanov M, Umeda M, Dowhan W. Phospholipid-assisted refolding of an integral membrane protein. Minimum structural features for phosphatidylethanolamine to act as a molecular chaperone. J Biol Chem. 1999; 274:12339–12345. [PubMed: 10212204]
7. Sedlák E, Robinson NC. Phospholipase A_2 digestion of cardiolipin bound to bovine cytochrome *c* oxidase alters both activity and quaternary structure. Biochemistry. 1999; 38:14966–14972. [PubMed: 10555978]
8. Valiyaveetil FI, Zhou Y, MacKinnon R. Lipids in the structure, folding, and function of the KcsA K^+ channel. Biochemistry. 2002; 41:10771–10777. [PubMed: 12196015]

9. Lange C, Nett JH, Trumpower BL, Hunte C. Specific roles of protein-phospholipid interactions in the yeast cytochrome bc1 complex structure. EMBO J. 2001; 20:6591–6600. [PubMed: 11726495]
10. Awasthi YC, Chuang TF, Keenan TW, Crane FL. Tightly bound cardiolipin in cytochrome oxidase. Biochim Biophys Acta. 1971; 226:42–52. [PubMed: 4323697]
11. Gomez B Jr, Robinson NC. Phospholipase digestion of bound cardiolipin reversibly inactivates bovine cytochrome bc1. Biochemistry. 1999; 38:9031–9038. [PubMed: 10413476]
12. Robinson NC. Specificity and binding affinity of phospholipids to the high affinity cardiolipin sites of beef heart cytochrome *c* oxidase. Biochemistry. 1982; 21:184–188. [PubMed: 6277366]
13. Schagger H, Hagen T, Roth B, Brandt U, Link TA, von Jagow G. Phospholipid specificity of bovine heart bc_1 complex. Eur J Biochem. 1990; 190:123–130. [PubMed: 2163831]
14. Zhang H, Kurisu G, Smith JL, Cramer WA. A defined protein-detergent-lipid complex for crystallization of integral membrane proteins: The cytochrome b6f complex of oxygenic photosynthesis. Proc Natl Acad Sci U S A. 2003; 100:5160–5163. [PubMed: 12702760]
15. Garavito RM, Ferguson-Miller S. Detergents as tools in membrane biochemistry. J Biol Chem. 2001; 276:32403–32406. [PubMed: 11432878]
16. Guan L, Smirnova IN, Verner G, Nagamori S, Kaback HR. Manipulating phospholipids for crystallization of a membrane transport protein. Proc Natl Acad Sci U S A. 2006; 103:1723–1726. [PubMed: 16446422]
17. Hosler JP, Ferguson-Miller S, Mills DA. Energy transduction: proton transfer through the respiratory complexes. Annu Rev Biochem. 2006; 75:165–187. [PubMed: 16756489]
18. Mills DA, Ferguson-Miller S. Understanding the mechanism of proton movement linked to oxygen reduction in cytochrome c oxidase: lessons from other proteins. FEBS Lett. 2003; 545:47–51. [PubMed: 12788491]
19. Marsh D, Horvath LI. Structure, dynamics and composition of the lipid- protein interface. Perspectives from spin-labelling. Biochim Biophys Acta. 1998; 1376:267–296. [PubMed: 9804973]
20. Powell GL, Knowles PF, Marsh D. Spin-label studies on the specificity of interaction of cardiolipin with beef heart cytochrome oxidase. Biochemistry. 1987; 26:8138–8145. [PubMed: 2831938]
21. Distler AM, Allison J, Hiser C, Qin L, Hilmi Y, Ferguson-Miller SM. Mass spectrometric detection of protein, lipid and heme components of cytochrome *c* oxidase from *R. sphaeroides* and the stabilization of non-covalent complexes from the enzyme. Eur Mass Spectrom. 2004; 10:295–308.
22. Svensson-Ek M, Abramson J, Larsson G, Tornroth S, Brzezinski P, Iwata S. The x-ray crystal structures of wild-type and EQ(I-286) mutant cytochrome *c* oxidases from *Rhodobacter sphaeroides*. J Mol Biol. 2002; 321:329–339. [PubMed: 12144789]
23. Fyfe PK, Isaacs NW, Cogdell RJ, Jones MR. Disruption of a specific molecular interaction with a bound lipid affects the thermal stability of the purple bacterial reaction centre. Biochim Biophys Acta, Bioenerg. 2004; 1608:11–22.
24. Palsdottir H, Hunte C. Lipids in membrane protein structures. Biochim Biophys Acta, Biomembr. 2004; 1666:2–18.
25. Zhang M, Mileykovskaya E, Dowhan W. Gluing the respiratory chain together. Cardiolipin is required for supercomplex formation in the inner mitochondrial membrane. J Biol Chem. 2002; 277:43553–43556. [PubMed: 12364341]
26. Pfeiffer K, Gohil V, Stuart Rosemary A, Hunte C, Brandt U, Greenberg Miriam L, Schagger H. Cardiolipin stabilizes respiratory chain supercomplexes. J Biol Chem. 2003; 278:52873–52880. [PubMed: 14561769]
27. Sorice M, Manganelli V, Matarrese P, Tinari A, Misasi R, Malorni W, Garofalo T. Cardiolipin-enriched raft-like microdomains are essential activating platforms for apoptotic signals on mitochondria. FEBS Lett. 2009; 583:2447–2450. [PubMed: 19616549]
28. Tyurin VA, Tyurina YY, Ritov VB, Lysytsya A, Amoscato AA, Kochanek PM, Hamilton R, Dekosky ST, Greenberger JS, Bayir H, Kagan VE. Oxidative lipidomics of apoptosis: quantitative assessment of phospholipid hydroperoxides in cells and tissues. Methods Mol Biol. 2010; 610:353–374. [PubMed: 20013189]

29. Sparagna GC, Chicco AJ, Murphy RC, Bristow MR, Johnson CA, Rees ML, Maxey ML, McCune SA, Moore RL. Loss of cardiac tetralinoleoyl cardiolipin in human and experimental heart failure. J Lipid Res. 2007; 48:1559–1570. [PubMed: 17426348]
30. Chang S-C, Heacock PN, Mileykovskaya E, Voelker DR, Dowhan W. Isolation and characterization of the gene (CLS1) encoding cardiolipin synthase in Saccharomyces cerevisiae. J Biol Chem. 1998; 273:14933–14941. [PubMed: 9614098]
31. Tuller G, Hrastnik C, Achleitner G, Schiefthaler U, Klein F, Daum G. YDL142c encodes cardiolipin synthase (Cls1p) and is non-essential for aerobic growth of Saccharomyces cerevisiae. FEBS Lett. 1998; 421:15–18. [PubMed: 9462830]
32. Jiang F, Rizavi HS, Greenberg ML. Cardiolipin is not essential for the growth of Saccharomyces cerevisiae on fermentable or non-fermentable carbon sources. Mol Microbiol. 1997; 26:481–491. [PubMed: 9402019]
33. Sistrom WR. A requirement for sodium in the growth of Rhodopseudomonas spheroides. J Gen Microbiol. 1960; 22:778–785. [PubMed: 14447230]
34. Sistrom WR. The kinetics of the synthesis of photopigments in Rhodopseudomonas spheroides. J Gen Microbiol. 1962; 28:607–616. [PubMed: 13913485]
35. Benning C, Somerville CR. Isolation and genetic complementation of a sulfolipid-deficient mutant of *Rhodobacter sphaeroides*. J Bacteriol. 1992; 174:2352–2360. [PubMed: 1551852]
36. Zhen Y, Qian J, Follmann K, Hayward T, Nilsson T, Dahn M, Hilmi Y, Hamer AG, Hosler JP, Ferguson-Miller S. Overexpression and purification of cytochrome c oxidase from Rhodobacter sphaeroides. Protein Expression Purif. 1998; 13:326–336.
37. van Niel CB. The Culture, General Physiology, Morphology, and Classification of the Non-Sulfur Purple and Brown Bacteria. Bacteriol Rev. 1944; 8:1–118. [PubMed: 16350090]
38. Yeliseev AA, Kaplan S. TspO of rhodobacter sphaeroides. A structural and functional model for the mammalian peripheral benzodiazepine receptor. J Biol Chem. 2000; 275:5657–5667. [PubMed: 10681549]
39. Benning C, Beatty JT, Prince RC, Somerville CR. The sulfolipid sulfoquinovosyldiacylglycerol is not required for photosynthetic electron transport in *Rhodobacter sphaeroides* but enhances growth under phosphate limitation. Proc Natl Acad Sci U S A. 1993; 90:1561–1565. [PubMed: 8434018]
40. Simon R, Priefer U, Puehler A. Vector plasmids for in vivo and in vitro manipulations of gram-negative bacteria. Mol Genet Bact-Plant Interact, [Symp]. 1983:98–106.
41. Weissenmayer B, Geiger O, Benning C. Disruption of a gene essential for sulfoquinovosyldiacylglycerol biosynthesis in *Sinorhizobium meliloti* has no detectable effect on root nodule symbiosis. Mol Plant-Microbe Interact. 2000; 13:666–672. [PubMed: 10830266]
42. Arondel V, Benning C, Somerville CR. Isolation and functional expression in *Escherichia coli* of a gene encoding phosphatidylethanolamine methyltransferase (EC 2.1.1.17) from *Rhodobacter sphaeroides*. J Biol Chem. 1993; 268:16002–16008. [PubMed: 8340421]
43. Tamot, B. MS thesis. Department of Biochemistry and Molecular Biology, Michigan State University; 2006. Construction and characterization of a cardiolipin-deficient mutant in *Rhodobacter sphaeroides*.
44. Hosler JP, Fetter J, Tecklenburg MMJ, Espe M, Lerma C, Ferguson-Miller S. Cytochrome aa3 of Rhodobacter sphaeroides as a model for mitochondrial cytochrome c-oxidase. Purification, kinetics, proton pumping, and spectral analysis. J Biol Chem. 1992; 267:24264–24272. [PubMed: 1332949]
45. Smith PK, Krohn RI, Hermanson GT, Mallia AK, Gartner FH, Provenzano MD, Fujimoto EK, Goeke NM, Olson BJ, Klenk DC. Measurement of protein using bicinchoninic acid. Anal Biochem. 1985; 150:76–85. [PubMed: 3843705]
46. Qin L, Mills DA, Buhrow L, Hiser C, Ferguson-Miller S. A conserved steroid binding site in cytochrome *c* oxidase. Biochemistry. 2008; 47:9931–9933. [PubMed: 18759498]
47. Altschul SF, Madden TL, Schaffer AA, Zhang J, Zhang Z, Miller W, Lipman DJ. Gapped BLAST and PSI-BLAST: a new generation of protein database search programs. Nucleic Acids Res. 1997; 25:3389–3402. [PubMed: 9254694]

48. Shibuya I, Miyazaki C, Ohta A. Alteration of phospholipid composition by combined defects in phosphatidylserine and cardiolipin synthases and physiological consequences in Escherichia coli. J Bacteriol. 1985; 161:1086–1092. [PubMed: 2982784]
49. Nishijima S, Asami Y, Uetake N, Yamagoe S, Ohta A, Shibuya I. Disruption of the Escherichia coli cls gene responsible for cardiolipin synthesis. J Bacteriol. 1988; 170:775–780. [PubMed: 2828323]
50. Zhang, X. PhD thesis. Department of Chemistry and Department of Biochemistry & Molecular Biology, Michigan State University; 2009. Investigating the functional roles of lipids in membrane protein cytochrome *c* oxidase from *Rhodobacter sphaeroides* using mass spectrometry and lipid profile modification.
51. Klug RM, Benning C. Two enzymes of diacylglyceryl-O-4′-(N,N,N,-trimethyl)-homoserine biosynthesis are encoded by btaA and btaB in the purple bacterium *Rhodobacter sphaeroides*. Proc Natl Acad Sci U S A. 2001; 98:5910–5915. [PubMed: 11331765]
52. Busch KL. Chemical noise in mass spectrometry. Part III - more mass spectrometry/mass spectrometry. Spectroscopy (Duluth, MN, United States). 2003; 18:52–55.
53. Zhang X, Ferguson-Miller SM, Reid GE. Characterization of ornithine and glutamine lipids extracted from cell membranes of *Rhodobacter sphaeroides*. J Am Soc Mass Spectrom. 2009; 20:198–212. [PubMed: 18835523]
54. Hsu F-F, Turk J, Rhoades Elizabeth R, Russell David G, Shi Y, Groisman Eduardo A. Structural characterization of cardiolipin by tandem quadrupole and multiple-stage quadrupole ion-trap mass spectrometry with electrospray ionization. Journal of the American Society for Mass Spectrometry. 2005; 16:491–504. [PubMed: 15792718]
55. Sparagna GC, Johnson CA, McCune SA, Moore RL, Murphy RC. Quantitation of cardiolipin molecular species in spontaneously hypertensive heart failure rats using electrospray ionization mass spectrometry. J Lipid Res. 2005; 46:1196–1204. [PubMed: 15772420]
56. Hirschberg CB, Kennedy EP. Mechanism of the enzymatic synthesis of cardiolipin in Escherichia coli. Proc Natl Acad Sci U S A. 1972; 69:648–651. [PubMed: 4551982]
57. Han X, Yang J, Yang K, Zhao Z, Abendschein DR, Gross RW. Alterations in myocardial cardiolipin content and composition occur at the very earliest stages of diabetes: a shotgun lipidomics study. Biochemistry. 2007; 46:6417–6428. [PubMed: 17487985]
58. Chicco AJ, Sparagna GC. Role of cardiolipin alterations in mitochondrial dysfunction and disease. Am J Physiol. 2007; 292:C33–C44.
59. Yamaoka-Koseki S, Urade R, Kito M. Cardiolipins from rats fed different dietary lipids affect bovine heart cytochrome *c* oxidase activity. J Nutr. 1991; 121:956–958. [PubMed: 1646874]
60. Lopez-Lara IM, Sohlenkamp C, Geiger O. Membrane lipids in plant-associated bacteria: Their biosyntheses and possible functions. Mol Plant-Microbe Interact. 2003; 16:567–579. [PubMed: 12848422]
61. Schlame M, Greenberg ML. Cardiolipin synthase from yeast. Biochim Biophys Acta. 1997; 1348:201–206. [PubMed: 9370334]
62. Gaspar ML, Aregullin MA, Jesch SA, Nunez LR, Villa-Garcia M, Henry SA. The emergence of yeast lipidomics. Biochim Biophys Acta, Mol Cell Biol Lipids. 2007; 1771:241–254.
63. Zhong Q, Gohil VM, Ma L, Greenberg ML. Absence of cardiolipin results in temperature sensitivity, respiratory defects, and mitochondrial DNA instability independent of pet56. J Biol Chem. 2004; 279:32294–32300. [PubMed: 15169766]
64. Russell NJ, Harwood JL. Changes in the acyl lipid composition of photosynthetic bacteria grown under photosynthetic and non-photosynthetic conditions. Biochem J. 1979; 181:339–345. [PubMed: 115463]
65. Catucci L, Depalo N, Lattanzio VMT, Agostiano A, Corcelli A. Neosynthesis of cardiolipin in Rhodobacter sphaeroides under osmotic stress. Biochemistry. 2004; 43:15066–15072. [PubMed: 15554714]
66. Robinson NC, Zborowski J, Talbert LH. Cardiolipin-depleted bovine heart cytochrome *c* oxidase: binding stoichiometry and affinity for cardiolipin derivatives. Biochemistry. 1990; 29:8962–8969. [PubMed: 2176838]

67. Berry EA, Trumpower BL. Isolation of ubiquinol oxidase from Paracoccus denitrificans and resolution into cytochrome bc1 and cytochrome c-aa3 complexes. J Biol Chem. 1985; 260:2458–2467. [PubMed: 2982819]

68. Loll B, Kern J, Saenger W, Zouni A, Biesiadka J. Towards complete cofactor arrangement in the 3.0 Å resolution structure of photosystem II. Nature. 2005; 438:1040–1044. [PubMed: 16355230]

69. Jones MR. Lipids in photosynthetic reaction centres: Structural roles and functional holes. Progress in Lipid Research. 2007; 46:56–87. [PubMed: 16963124]

70. Aygun-Sunar S, Mandaci S, Koch H-G, Murray IVJ, Goldfine H, Daldal F. Ornithine lipid is required for optimal steady-state amounts of *c*-type cytochromes in *Rhodobacter capsulatus*. Mol Microbiol. 2006; 61:418–435. [PubMed: 16856942]

71. Laible PD, Scott HN, Henry L, Hanson DK. Towards higher-throughput membrane protein production for structural genomics initiatives. J Struct Funct Genomics. 2004; 5:167–172. [PubMed: 15263855]

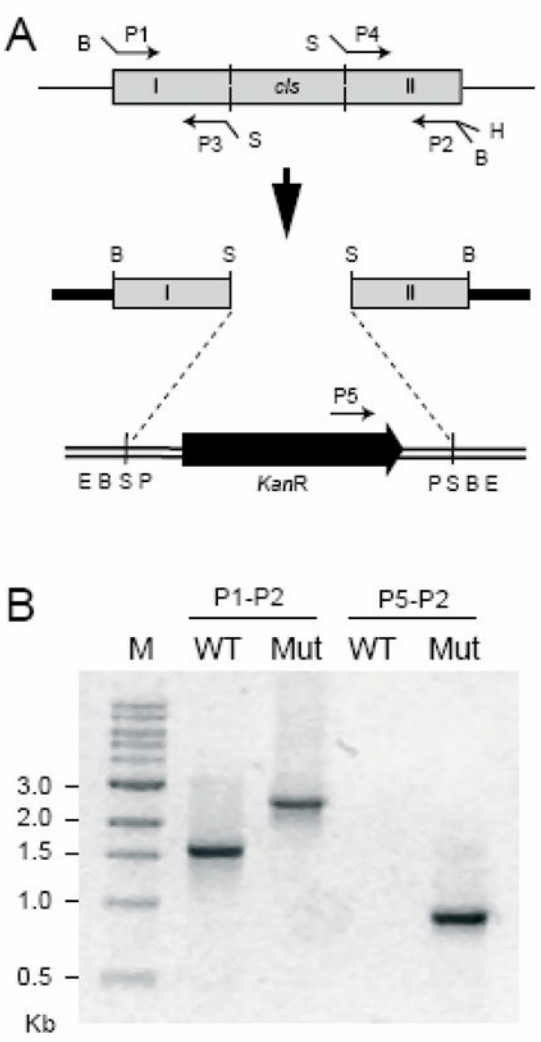

Figure 1.

Disruption of the *cls* gene. (A) Schematic diagram showing the gene disruption strategy. Grey boxes represent the *cls* gene and amplified segments of the gene. The black block arrow represents the kanamycin resistance cassette and the direction of the arrowhead shows its orientation. Plasmids pPICT-2 and pUC4K are shown as thick solid lines and double lines, respectively. Restriction sites: B, *Bam*HI; S, *Sal*I, H, *Hind*III; E, *Eco*RI; P, *Pst*I. (B) PCR verification for the gene disruption. Genomic DNA was isolated from the type (WT) and the *cls*-deleted mutant (Mut) strains and two PCR reactions were carried out using different sets of primers placed at the positions indicated in Fig. 2A. The sizes of the PCR products were compared by gel electrophoresis. M indicates the marker lane.

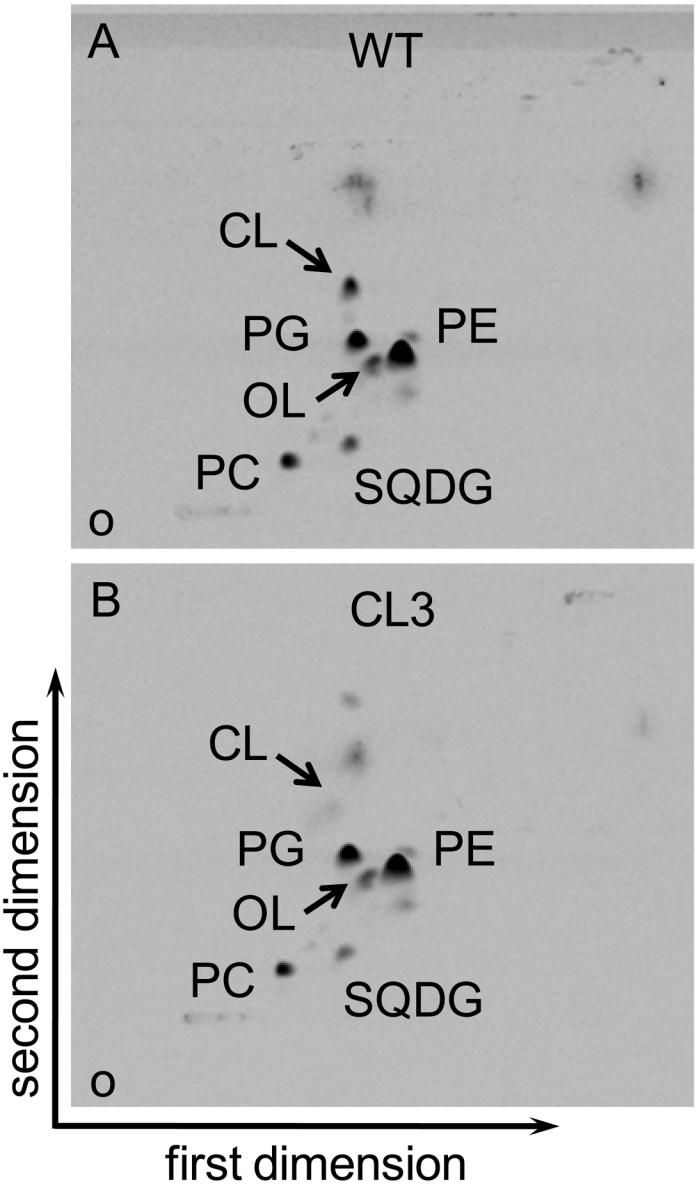

Figure 2.

Two-dimensional thin-layer chromatogram of ^{14}C-labeled lipids from the aerobically-grown *R. sphaeroides* (A) wild-type strain 2.4.1 and (B) the *cls*-deleted mutant CL3. The lipids were visualized by using a phosphoimager. Lipids: PE, phosphatidylethanolamine; PG, phosphatidylglycerol; PC, phosphatidylcholine; SQDG, sulfolipid; OL, ornithine lipid; CL, cardiolipin. O, origin.

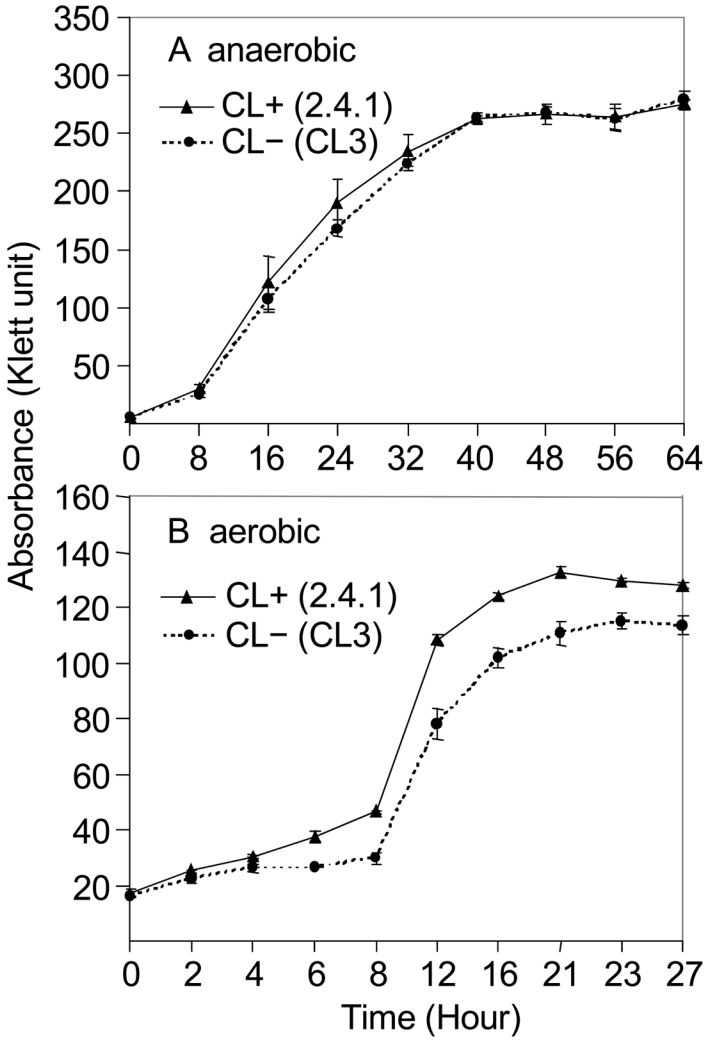

Figure 3.

Growth curves of *R. sphaeroides* wild-type (▲; 2.4.1) and CL-deficient mutant (●; CL3) strains under A) anaerobic photoheterotrophic growth, and B) aerobic chemoheterotrophic growth conditions, both in Sistrom's media at 30 °C. The data presented are the average of three independent growth cultures and the error bars are the standard deviations. Absorbances are expressed in Klett units, where 1 Klett unit is equivalent to 10^7 cells per mL (38).

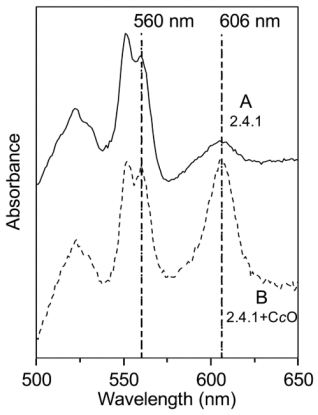

Figure 4.

Optical difference spectra of dithionite-reduced minus ferricyanide-oxidized solubilized membranes from A) *R. sphaeroides* strains 2.4.1 (wild-type) and B) 2.4.1+C*c*O (wild-type with C*c*O genes added on the expression plasmid PRK- pYJ123H). The relative levels of C*c*O are indicated by the sizes of the *a*-type heme absorbance peaks at 606 nm compared to the b-heme at 560 nm. The spectra are normalized to the 560 nm (*b*-type heme) peak. (Note that these membranes also contain the *bc*1 complex, a *cbb*3 type oxidase, and a membrane-bound cytochrome *c* which all contribute to the 560 nm and 550 nm peaks.)

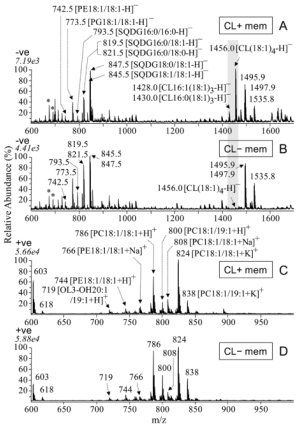

Figure 5.

MALDI-MS spectra of membranes isolated from CL(+) (169WT) and CL(−) (169CL3) strains of *R. sphaeroides* in negative ion mode (A and B) and in positive ion mode (C and D). The highlighted peaks in A) are those of CL at 1456, 1430, and 1428, which are barely discernable in B), the CL(–) sample. A) CL(+) membranes in negative ion mode, B) CL(−) membranes in negative ion mode, C) CL(+) membranes in positive ion mode, D) CL(−) membranes in positive ion mode, each at 0.25 mg/mL membrane protein concentration. The identities of labeled ions in each spectrum were confirmed by MS/MS experiments. Ions labeled with asterisks were identified as 2,5-DHB matrix cluster adducts. The peaks at m/z 1495.9, 1497.9, 1533.8 and 1535.8 were determined by MS/MS and MS^n not to be CL or CL derivatives.

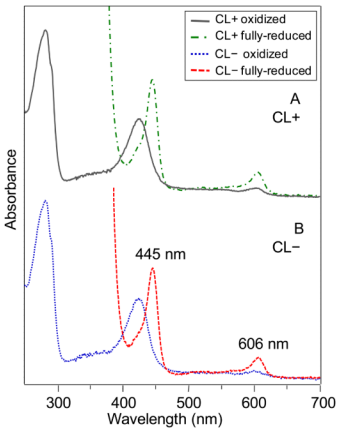

Figure 6.

Oxidized and reduced spectra of purified C*c*O samples used to produce protein crystals, purified from A) CL(+) (169WT) and B) CL(−) (169CL3) strains grown aerobically at 30 ºC. The reduced peaks at 445 and 606 nm, which are characteristic of the native heme *a* and a_3 spectra, are seen to be at the same wavelengths in both C*c*O forms. These peaks have contributions of both hemes at both wavelengths. The spectra were acquired using the same C*c*O protein concentrations.

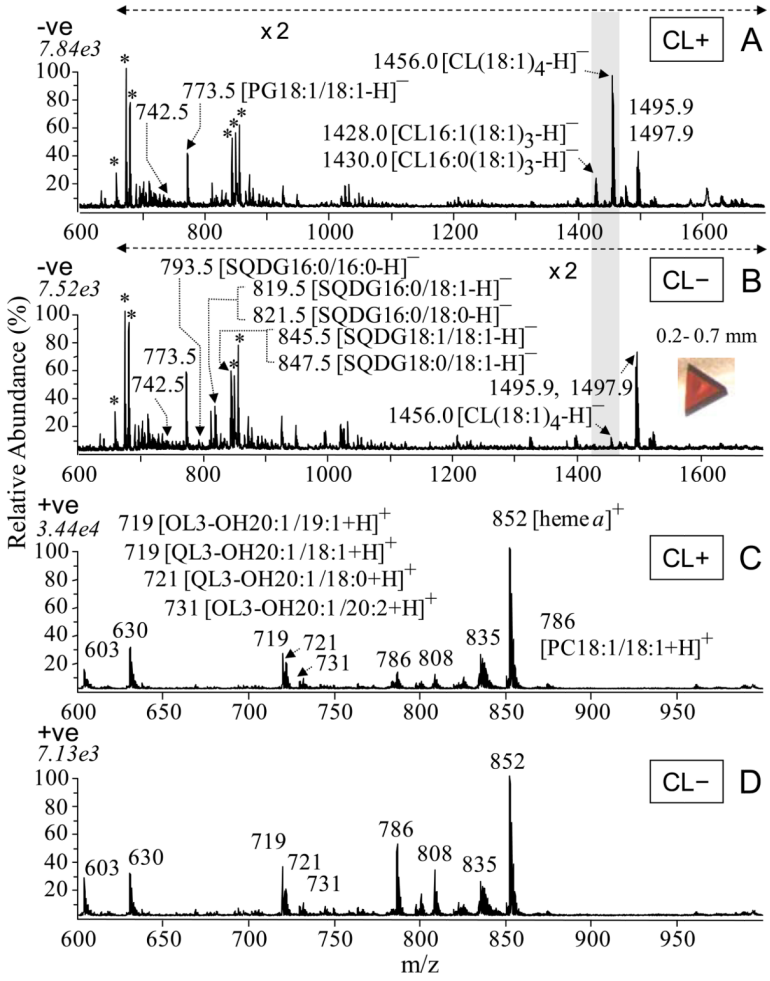

Figure 7.

MALDI-MS spectra of the four-subunit C*c*O protein crystals from CL(+) (169WT) and CL(−) (169CL3) strains of *R. sphaeroides* in negative ion mode (A and B) and positive ion mode (C and D), showing a marked difference in CL content by relative peak height at m/z 1456 (highlighted). A) C*c*O from CL(+) in negative ion mode, B) C*c*O from CL(−) in negative ion mode, C) C*c*O from CL(+) in positive ion mode, D) C*c*O from CL(−) in positive ion mode. Ions labeled with asterisks were identified as 2,5-DHB matrix cluster adducts. The identities of labeled ions in each spectrum were confirmed by MS/MS experiments. Inset in B: photo of a typical four-subunit C*c*O crystal used in this analysis.

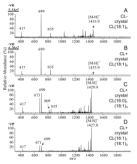

Figure 8.

Identification of the cardiolipin molecular species in the four-subunit C*c*O crystals from CL(+) (169WT) and CL(−) (169CL3) *R. sphaeroides* using CID MS/MS in negative ion mode on a MALDI-linear ion trap mass spectrometer, showing the marked depletion of $CL(18:1)_4$ in CL(−) crystals compared to CL(+) crystals (A and B) as demonstrated by comparison of the absolute ion abundance of m/z 699 (top left of panels A and B), the predominant product ion generated by $CL(18:1)_4$ in MS/MS, corresponding to the phosphatidyldioleoylglyceride moiety. The figure identifies multiple CL species in CL(+) C*c*O crystals (B, C, D) but no CL $(18:2)_4$ at m/z 1448 is seen (see also Figure 7A).

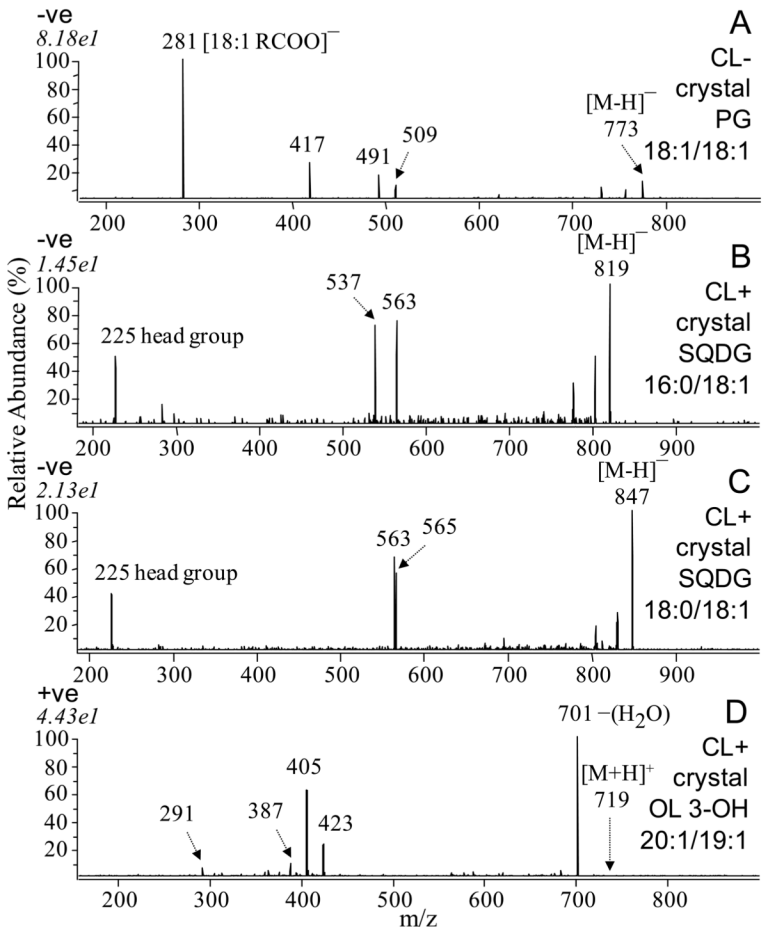

Figure 9.

MS/MS spectra showing the characteristic fragmentation patterns of the precursor ions of the major lipids, providing the identifications of these lipids in the C*c*O crystals from CL(+) (169WT) and CL(−) (169CL3) *R. sphaeroides* using CID MS/MS in positive and negative ion modes on a MALDI-linear ion trap mass spectrometer. Representative lipids in the crystals include A) PG 18:1/18:1 at m/z 773 (−ve), B) SQDG 16:0/18:1 at m/z 819 (−ve), C) SQDG 18:0/18:1 at m/z 847 (−ve) and D) OL 3-OH 20:1/19:1 at m/z 719 (+ve). In panels B and C, the fragment ion at m/z 225 is determined by MS^3 to represent the sulfoquinovosyl head group of SQDG, and the peaks in the middle of the spectra are generated by the neutral loss of either one of the two fatty acid chains respectively.

Table 1

Lipid composition of *R. sphaeroides* wild-type (2.4.1) and CL-deficient mutant (CL3) determined by thin-layer chromatograpy and radioactive labeling

Lipid	wild-type	CL3
CL	5.6 ± 1.6	0.5 ± 0.1
OL	3.7 ± 0.2	3.5 ± 0.4
PE	42.4 ± 4.3	44.1 ± 2.5
PG	22.4 ± 0.1	26.2 ± 2.2
SQDG	6.7 ± 0.2	6.4 ± 1.3
PC	19.2 ± 4.4	19.2 ± 3.8

Keys: The values given represent the mean percentage of radioactivity for individual lipids ± the standard error from 3 independent experiments. CL, cardiolipin; PE, phosphatidylethanolamine; OL, ornithine lipid; PG, phosphatidylglycerol; SQDG, sulfoquinovosyldiacylglycerol; PC, phosphatidylcholine.

Table 2

Spectral and enzymatic properties of C*c*O purified from *R. sphaeroides* wild-type (2.4.1+C*c*O) and cardiolipin-depleted (CL3+C*c*O) cell lines

Cell Line	Genotype	Spectral Peaks of Purified C*c*O (nm)		Activity (s^{-1}) no added lipid	Activity (s^{-1}) plus added lipid	Increase in activity with lipid
		Soret	Alpha			
2.4.1+C*c*O	wild-type	445	606	1050 ± 100[#]	1340 ± 50[#]	28 ± 2%[#]
CL3 +C*c*O	Δ*cls*	445	606	1060 ± 109[@]	1410 ± 120[@]	33 ± 8%[@]

Keys: Both strains produced his-tagged C*c*O from a plasmid (PRK-pYJ123H (36)). The Soret and alpha peaks were from the optical spectra of dithionite-reduced C*c*O. The molecular activity of purified C*c*O was measured at pH 6.5 and presented as turnover number (moles cytochrome *c* oxidized per mole C*c*O per second). The number of independent measurements was 3[#] or 5[@].